

NUSC Technical Report 8323
7 September 1988

①

DTIC FILE COPY

AD-A204 007

Global Model for Sound Absorption in Sea Water: Impact Study Part I

P. M. Schelfele
Combat Systems Analysis Staff

R. H. Mellen
OMNI Analysis

D. G. Browning
Advanced Concepts Office



DTIC
ELECTE
24 JAN 1989
S D
RE

Naval Underwater Systems Center
Newport, Rhode Island / New London, Connecticut

Approved for public release; distribution is unlimited.

89 1 23 207

REPORT DOCUMENTATION PAGE

1a. REPORT SECURITY CLASSIFICATION UNCLASSIFIED		1b. RESTRICTIVE MARKINGS	
2a. SECURITY CLASSIFICATION AUTHORITY		3. DISTRIBUTION / AVAILABILITY OF REPORT Approved for public release; distribution is unlimited.	
2b. DECLASSIFICATION / DOWNGRADING SCHEDULE			
4. PERFORMING ORGANIZATION REPORT NUMBER(S) NUSC Technical Report 8323		5. MONITORING ORGANIZATION REPORT NUMBER(S)	
6a. NAME OF PERFORMING ORGANIZATION Naval Underwater Systems Center	6b. OFFICE SYMBOL (If applicable) 61M	7a. NAME OF MONITORING ORGANIZATION	
6c. ADDRESS (City, State, and ZIP Code) New London Laboratory New London, CT 06378		7b. ADDRESS (City, State, and ZIP Code)	
8a. NAME OF FUNDING / SPONSORING ORGANIZATION Naval Underwater Systems Center	8b. OFFICE SYMBOL (If applicable) 10	9. PROCUREMENT INSTRUMENT IDENTIFICATION NUMBER	
8c. ADDRESS (City, State, and ZIP Code) New London Laboratory New London, CT 06320		10. SOURCE OF FUNDING NUMBERS	
		PROGRAM ELEMENT NO.	PROJECT NO. 710Y11
11. TITLE (Include Security Classification) GLOBAL MODEL FOR SOUND ABSORPTION IN SEA WATER: IMPACT STUDY PART I			
12. PERSONAL AUTHOR(S) P. M. Scheifele, D. G. Browning, and R. H. Mellen (OMNI Analysis)			
13a. TYPE OF REPORT Summary	13b. TIME COVERED FROM TO	14. DATE OF REPORT (Year, Month, Day) 1988 September 7	15. PAGE COUNT 31
16. SUPPLEMENTARY NOTATION			
17. COSATI CODES		18. SUBJECT TERMS (Continue on reverse if necessary and identify by block number) Sound Absorption	
FIELD	GROUP SUB-GROUP		
19. ABSTRACT (Continue on reverse if necessary and identify by block number) NUSC Technical Report 8323 contains the unclassified portion of "Global Model for Sound Absorption in Sea Water: Impact Study, Part I." NUSC Technical Report 8325 contains the confidential portion of this study.			
20. DISTRIBUTION / AVAILABILITY OF ABSTRACT <input type="checkbox"/> UNCLASSIFIED/UNLIMITED <input checked="" type="checkbox"/> SAME AS RPT <input type="checkbox"/> OTIC USERS		21. ABSTRACT SECURITY CLASSIFICATION UNCLASSIFIED	
22a. NAME OF RESPONSIBLE INDIVIDUAL D. G. Browning		22b. TELEPHONE (Include Area Code) (203) 440-4173	22c. OFFICE SYMBOL 304

TABLE OF CONTENTS

page

Summary.....ii

Background.....1

Absorption Model.....2

PH Profiles.....7

Global Model.....8

K Profiles.....9

Convergence Zone Mode.....10

Bottom Bounce Mode.....11

Surface Duct Mode.....15

References.....20

Appendix A: K Contours.....21

Accession For	
NTIS GRA&I	<input checked="" type="checkbox"/>
DTIC TAB	<input type="checkbox"/>
Unannounced	<input type="checkbox"/>
Justification	
By	
Distribution/	
Availability Codes	
Dist	

A-1



Summary

Analysis of propagation loss is generally based on the absorption formula developed by Thorp in 1965. The Global Model is an improved formula based on more recent field and laboratory experiments. The new formula involves the pH factor $K=10^{(pH-8)}$, which varies with both region and depth. In order to account for depth variation, the effective absorption must be calculated by integrating loss over ray paths. Contour charts are provided for estimating the required K profiles throughout the World Ocean.

The purpose of this report is to examine the impact of the model on sonar performance and the surface and bottom-loss models upon which predictions are currently based. The present analysis is limited mainly to active systems operating in the frequency range 3-4 kHz. The four regions examined are: North Atlantic, North Pacific, Eastern Mediterranean and Norwegian Sea.

Comparison of K model predictions with those based on the Thorp formula indicates that two-way path absorption for the first CZ zone ranges from approximately 4 dB less in the North Pacific to 12 dB greater in the Eastern Mediterranean. In the bottom-bounce mode, these values are reduced roughly in proportion to range.

The MGS bottom-loss model is based on analysis of one-way paths using the Thorp formula. The difference between the K model and Thorp formula for 10° grazing angle in the Eastern Mediterranean is roughly 4 dB, making the actual bottom-loss smaller by about one province number. The differences decrease with increasing grazing angle and are smaller in the other areas. Corrections to the MGS model should therefore be relatively minor.

K model predictions of two-way loss for the surface-duct mode at 25 km range vary from 3 to 8 dB more than Thorp values, since pH tends to be high near the surface. The higher absorption coefficients evidently account for a large fraction of the excess attenuation previously ascribed to surface loss. Since the surface-loss models were based on pre-Thorp absorption models, a major reassessment is indicated.

Background

Sound absorption in sea water is more than an order of magnitude greater than in fresh water. The excess is the result of relaxations involving certain chemical constituents. Laboratory experiments in the 1950's identified the principle mechanism as a magnesium sulfate with relaxation frequency near 100 kHz. Combining measured relaxation parameters with data from field experiments in the frequency range 2-30 kHz, Schulkin and Marsh [1] devised the first practical formula for sound absorption in sea water in 1962.

At about that time, interest shifted to lower frequencies in an effort to increase range and questions arose about extrapolation of the S&M formula. In 1965, Thorp [2] reported results of long-range sound-channel experiments covering lower frequencies and a second anomaly was observed. The data were fitted by adding a 1 kHz relaxation component to the S&M formula and this became known as the "Thorp formula" [3].

Mediterranean experiments by Leroy [4], showed a similar anomaly with greater magnitude and relaxation frequency. Experiments carried over the next two decades in other areas confirmed the variability of the anomaly and regional dependence became a critical factor

The anomaly was identified as a second relaxation involving boric acid, a minor sea-water constituent [5]. In this case, absorption depends on pH as well as temperature [6]. The relaxation mechanism was identified as the boric acid/carbonate equilibrium and parameters were measured in the laboratory [7]. The experiments also showed that a pH-dependent relaxation of magnesium carbonate has a minor but significant role in sea water absorption [8].

An absorption formula, based solely on known chemical processes, would be too complex and the accuracy would be inadequate as well. However, the range of the ocean parameters is small and simplifying approximations can be made; i.e. that magnitudes of pH-dependent terms increase exponentially with pH and that relaxation frequency increases exponentially with the temperature. The Thorp formula can then be modified by simply adding the third relaxation and including pH and temperature factors for all terms.

A 3-relaxation formula has been developed and absorption coefficients based on archival pH values have been found to be in good agreement with experimental data. For prediction purposes, the Global Model [9] includes contour charts for estimating pH correction factors vs depth as well as region. The purpose of this report is to examine the potential impact of the model on systems performance and the surface and bottom-loss models upon which predictions are currently based.

Absorption Model

$A = A_1(\text{MgSO}_4) + A_2(\text{B}(\text{OH})_3) + A_3(\text{MgCO}_3)$ $A_n = (S/35) a_n F^2 F_n / (F_n^2 + F^2)$	
$a_1 = 0.5 \times 10^{-D(\text{km})/20}$	$F_1 = 50 \times 10^{T/60}$
$a_2 = 0.1 \times 10^{(\text{pH}-8)}$	$F_2 = 0.9 \times 10^{T/70}$
$a_3 = 0.03 \times 10^{(\text{pH}-8)}$	$F_3 = 4.5 \times 10^{T/30}$
Atlantic 4°C pH 8.0 $A = 0.007f^2 + 0.1f^2/(1+f^2) + 0.18f^2/(6^2+f^2)$	
N.Pacific 4°C pH 7.7 $A = 0.007f^2 + 0.05f^2/(1+f^2) + 0.09f^2/(6^2+f^2)$	
Mediterranean Sea 14°C pH 8.3 $A = 0.006f^2 + 0.26f^2/(1.4^2+f^2) + 0.78f^2/(12^2+f^2)$	
Norwegian Sea 0°C pH 8.2 $A = 0.01f^2 + 0.16f^2/(0.9^2+f^2) + 0.2f^2/(4.5^2+f^2)$	

Table 1: Simplified absorption formulae.

Relaxational absorption formula have the simple form shown in the top box of Table 1. Values are for A in dB/km, F and relaxation frequency F_n in kHz and T in °C. The 3 components of the model are simply additive. Thorp's value pH=8.0 is used as reference. The pure water term is omitted, making the formula valid for frequencies less than roughly 100 kHz. Values of pH in the World Ocean vary roughly from 7.7 to 8.3, corresponding to an absorption ratio of almost 4/1 at the lower frequencies.

The magnesium sulfate term (A1) also includes the depth factor D(km), which is adopted from the pressure correction of Fisher and Simmons [10]. Depth dependencies of the other relaxations are not yet known; however, the field data indicate that effects on the boric acid term (A2) are negligible. Effects on the magnesium carbonate term (A3) will be much less important because its contribution is so small.

Specific formulae are shown in the bottom box. Note that the A1 terms are approximations valid only for $F \ll F_1$.

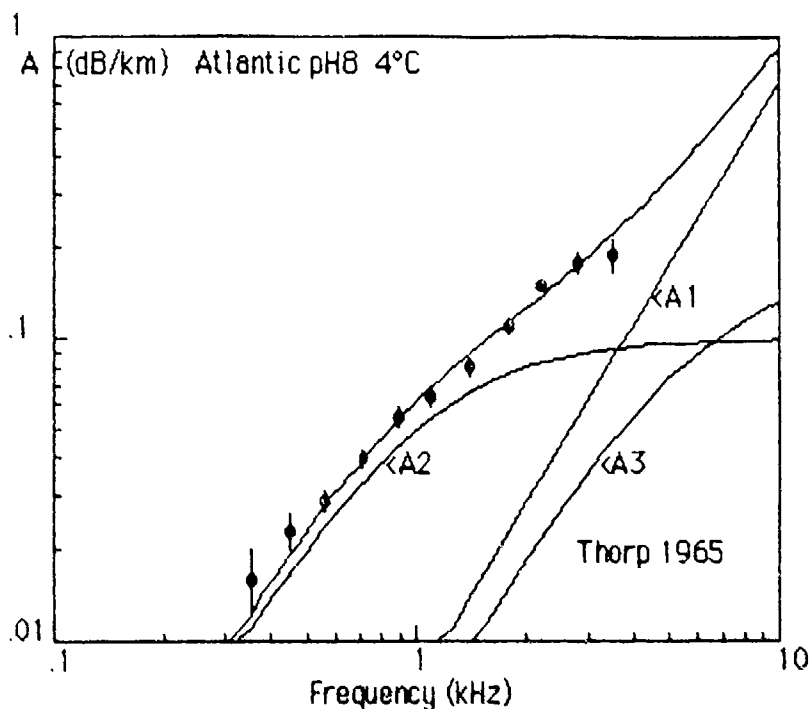


Figure 1: Thorp's data and 3-relaxation model.

Thorp's formula for the N. Atlantic sound channel was given as [3].

$$\alpha = 40 F^2 / (4100 + F^2) + 0.1 F^2 / (1 + F^2) \text{ dB/kyd.}$$

Note that the temperature and depth terms in the S&M formula are omitted and therefore it applies strictly to roughly 4°C at 1 km depth.

Figure 1 shows Thorp's original data compared to the 3-relaxation model. The individual components are identified and the top curve is their sum. The overall fit to the data is as good or better than the 2-component formula. Note that the boric acid (A2) coefficient is lower than that in the Thorp formula by some 10%, making the coefficient in dB/km becomes equal to the coefficient of the second term in Thorp's equation. The magnesium carbonate component makes up the difference at the lower frequencies.

The parameter adjustment in the present model is mainly justified on the basis of data-fit, the third component having been found essential. When the laboratory data were fitted by a 2-relaxation model, serious discrepancies appeared at higher pH values. For example, correcting Thorp's second term to pH 5 gave values that much too low in the 10 kHz range, clear evidence of another component. By sea-water synthesis, the mechanism was identified as magnesium carbonate, temperature and pH dependence of the parameters were measured and the relaxation incorporated as the third component of the absorption model.

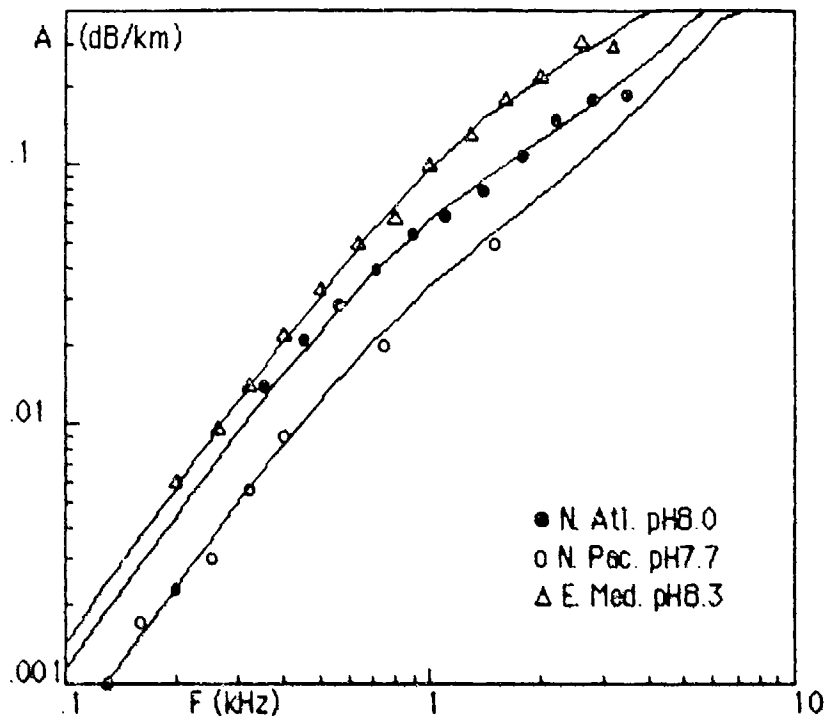


Figure 2: Model and data comparison.

Figure 2 compares the 3-component relaxation model predictions and data from sound-channel experiments in the Mediterranean, North Pacific and North Atlantic (Thorp).

In the North Pacific case, the lower value $\text{pH} \approx 7.7$ reduces both the boric acid (A2) and the magnesium carbonate (A3) coefficients by a factor of two compared to the N. Atlantic values. Relaxation frequency depends only on the temperature and remains the same.

In the Mediterranean case, the higher value $\text{pH} \approx 8.3$ increases both the boric acid (A2) and the magnesium carbonate (A3) coefficients by a factor of two compared to the N. Atlantic. However, the relaxation frequency is higher and the curves do not differ by as large a factor at the lower frequencies.

The value $\text{pH} 8.0$ has been assumed for Thorp's sound-channel experiment and is used as reference value for the 3-relaxation model. Predictions based on archival pH values then show good agreement within experimental limits for all regions examined.

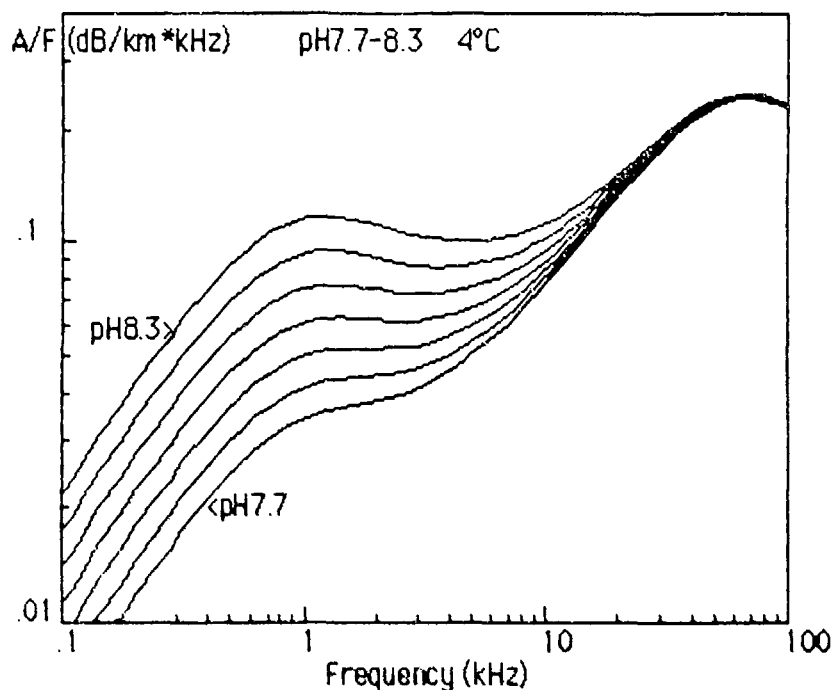


Figure 3: Absorption spectra A/F vs pH for T=4°C.

The effects of the 3-relaxation model are illustrated in Figures 3 and 4. Note that the absorption coefficient A has been divided by the frequency F(kHz) in order to compress the vertical scale.

Predicted spectra vs pH for 4°C and normal salinity (S=35) are shown in Figure 3 and cover the approximate sea-water range of pH 7.7-8.3 in 0.1 steps. The effect of pH on the absorption spectrum below 10 kHz is mainly due to the coefficient of the boric acid component A₂. Below 1 kHz, the max/min ratio approaches the factor four.

From analysis of experimental data, the overall error of the model is estimated to be roughly of the order of ±15%. In other words, the RMS error of an estimated coefficient in dB/km is not expected to be any greater if not limited by the accuracy of the environmental factors. For example, a change of 0.05 pH units corresponds to a 12% change in the boric acid coefficient and the pH error must be within these limits in order to realize the model accuracy. A major limiting factor is therefore the accuracy of the pH data-base.

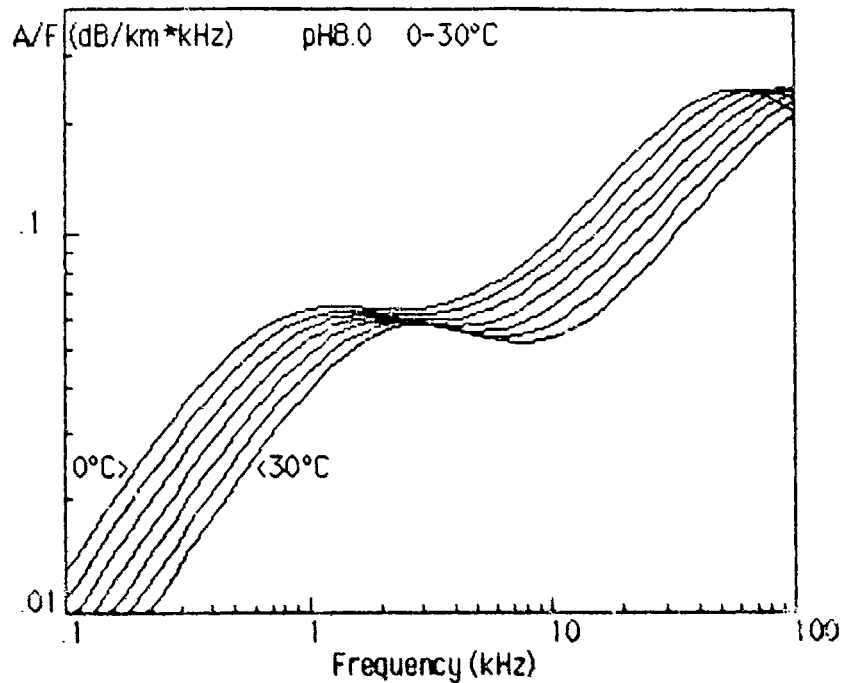


Figure 4: Absorption spectra A/F vs temperature for pH 8.0.

Figure 4 shows the predicted spectrum dependence on temperature for pH=8.0 and normal salinity ($S=35$), covering the nominal sea-water range $C=30^{\circ}C$ in $5^{\circ}C$ steps.

Temperature effects in the model come about only through the relaxation frequency coefficients of the three terms. Increasing temperature shifts the curves upward in frequency.

Model errors involving temperature coefficient are estimated to be within the expected $\pm 15\%$ limits. Since the temperature sensitivity is rather low, the value need only be known only to within roughly $\pm 1^{\circ}C$ to be well within these limits.

Errors involved in the salinity factor are probably also within the accuracy limits for the normal sea-water range. Salinity variations are evidently the result of evaporation or dilution by fresh water. Concentrations of all the constituents, except carbon dioxide, tend to remain in constant ratio. Carbon dioxide concentration evidently tends to remain constant.

The multiplying factor $S/35$ for all three components may be justified over a limited range, say 30-40 ppt. Beyond this range, corrections must be made for changes in the boric acid relaxation frequency. This can require a more accurate knowledge of the concentrations, which is beyond the scope of the present model.

PH Profiles

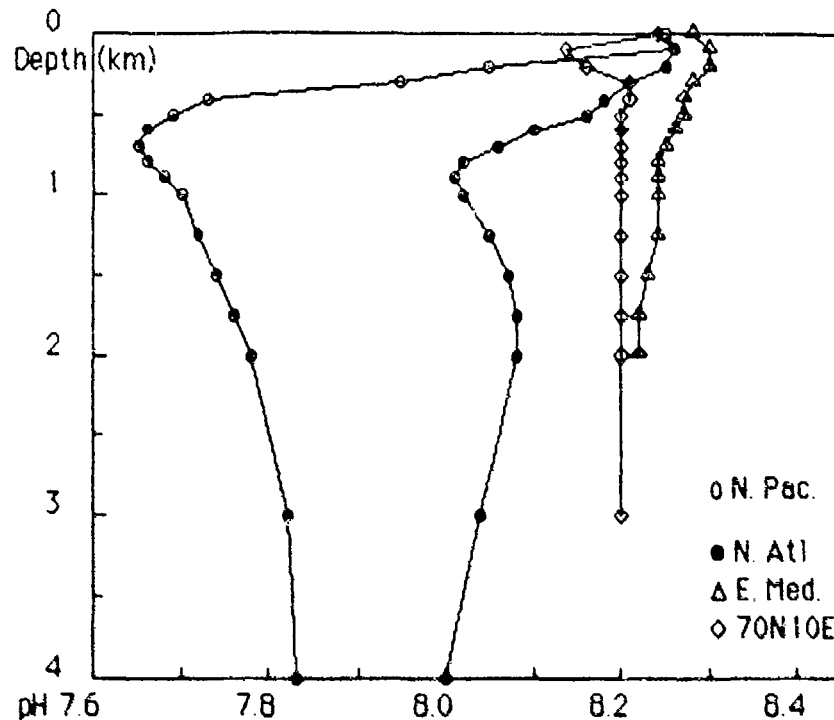


Figure 5: pH profiles.

In addition to regional variability, pH also can depend strongly on depth. Figure 5 compares pH profiles for various regions of the World Ocean. It is clear that the absorption will vary significantly for different ray paths, particularly in the North Pacific where sound-channel losses will be much less than for other paths. In order to account for the depth variability, the most general method of estimating effective absorption is to integrate loss over all the ray paths involved. This requires an appropriate profile for the pH factor. The Global Model uses contour charts of constant pH at 5 selected depths and the profile is generated by algorithm.

Contours of constant pH at selected depths from the World Ocean Atlases of Gorshkov [11] have been used in the analysis. The profile increments are 0.1 pH units and interpolation is required. *In-situ* pH values are used in the Global Model model and appropriate corrections have been made.

The GEOSECS reports [12] contain pH profiles obtained from circuits of the Atlantic, Pacific and Indian Oceans. These data have been used together with the Russian data to develop the constant-pH contour charts.

Global Model

$$A = A_1(\text{MgSO}_4) + A_2(\text{B}(\text{OH})_3) + A_3(\text{MgCO}_3)$$

$$A_n = (S/35) a_n F^2 F_n / (F_n^2 + F^2)$$

$a_1 = 0.5 \times 10^{-D(\text{km})/20}$	$F_1 = 50 \times 10^{T/60}$
$a_2 = 0.1 K$	$F_2 = 0.9 \times 10^{T/70}$
$a_3 = 0.03 K$	$F_3 = 4.5 \times 10^{T/30}$

Table 2: Global model absorption formula.

Variability of pH is clearly the major limiting factor in the accuracy of the absorption formula. In Table 2, the pH parameter $K = 10^{(\text{pH}-8)}$ has been substituted in the formula of Table 1.

Five K points have been found to give a reasonably accurate estimate of the K-profiles. The points are numbered 0-4 and the profile is fitted by the expression:

$$K(D) = K(4) + [C_0 + C_1 D + C_2 D^2 + C_3 D^3 + C_4 D^4] \exp[-(aD)^{1.5}]$$

where the exponent 1.5 has been chosen by trial to obtain "best" results. For latitudes less than 60°, the depth values $D=0, 0.5, 1, 2, \text{ and } 4$ km are used with $a=1/\text{km}$. Since water depths for latitudes greater than 60° are generally shallower and most of the variability of concern is concentrated nearer the surface, the depth values $D=0, 0.1, 0.3, 0.5, 1$ km are used with $a=4/\text{km}$.

The five equations for $n=0, 1, 2, 3, 4$ to be solved are then given by

$$C_0 + C_1 D_n + C_2 D_n^2 + C_3 D_n^3 + C_4 D_n^4 = [K(D_n) - K(4)] \exp[-(aD_n)^{1.5}]$$

and solution for the coefficients can be obtained either algebraically or by writing the equations in matrix form and inverting.

The K contour charts for the lower latitudes are shown in Appendix A, Figures 1A-5A. The high latitudes charts are shown in Figures 6A-11A and include surface values for both summer and winter conditions.

K Profiles

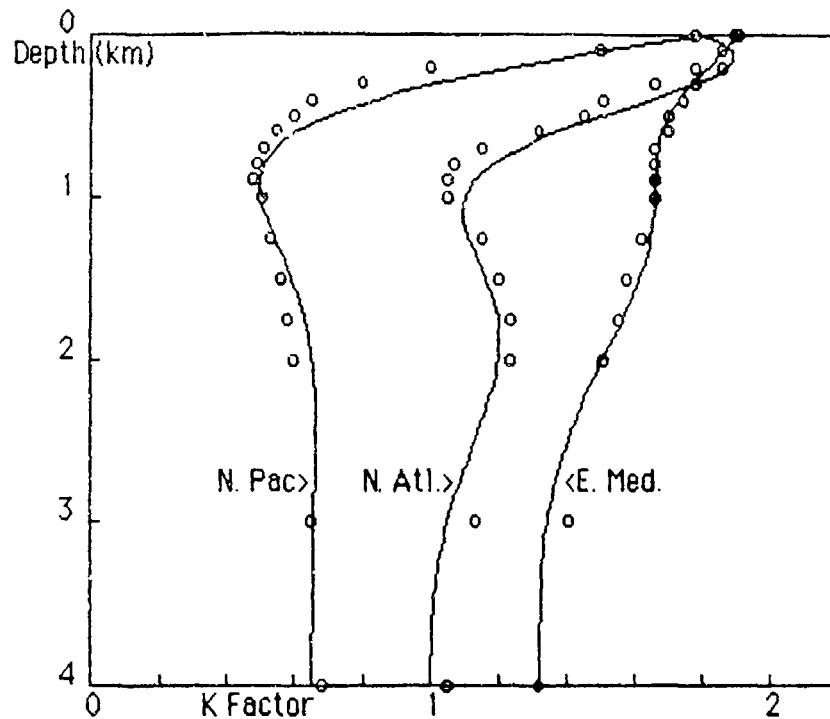


Figure 6: K profiles and data.

Figure 6 shows calculated profiles compared to typical data for the three regions. Errors are seen to be insignificant in comparison to the expected overall error of the model. The North Pacific and Eastern Mediterranean cases represent the expected extremes in ϕ effects.

Both K and temperature profiles are used for integrating absorption along the ray paths. The temperature profiles are generated in the same manner. Salinity is taken as constant $S=35$ except for the Mediterranean case where $S=38$ is used. Absorption at selected frequencies $F(\text{kHz})$ at ranges $R(\text{km})$ are calculated by integration over the appropriate ray paths for the convergence zone, bottom-reflection and surface duct modes. Note that total range along the ray paths is used throughout.

Expected errors are calculated concurrently using $\Delta K = \pm 0.05$ for the CZ and bottom-bounce modes and $\Delta K = \pm 0.1$ for the surface-duct mode. Values for the Thorp equation are also calculated concurrently so as to minimize relative errors. The values $\Delta = A(K_{\text{mod}}) - A(\text{Thorp})$ are the dB differences between the models and the $\pm \Delta$ values indicate the degree of significance of the K model.

Convergence Zone Mode

2Alpha (dB) CZ		Atl. 30°N	Pac. 45°N	E Med.	70N10E
F (kHz)	R (km)				
4.0	K mod.	43.6	29.8	33.3	26.7
	Thorp	40.4	33.8	21.1	21.1
	Δ	3.2±1.1	-4.0±0.9	12.1±0.7	5.5±0.6
3.5	K mod.	37.6	25.0	29.7	23.0
	Thorp	34.2	28.7	17.9	17.9
	Δ	3.4±1.0	-3.7±0.9	11.8±0.6	5.1±0.5
3.0	K mod.	32.0	20.7	26.2	19.5
	Thorp	26.7	24.1	15.0	15.0
	Δ	3.3±0.9	-3.4±0.8	11.2±0.6	4.5±0.5
2.5	K mod.	26.7	16.7	22.6	16.3
	Thorp	23.8	19.3	12.5	12.5
	Δ	2.9±0.8	-3.3±0.7	10.1±0.5	3.8±0.4
2.0	K mod.	21.5	13.0	18.5	13.2
	Thorp	19.2	16.1	10.1	10.1
	Δ	2.2±0.7	-3.1±0.6	8.4±0.4	3.1±0.4

Table 3: CZ two-way path absorption.

Calculations of two-way path absorption for CZ propagation in the four regions by the ray integration method are shown in Table 3.

Values for the N Atlantic indicate that the K model is roughly 3 dB higher than the Thorp formula ($\Delta \approx 3$ dB) in the 3-4 kHz range. This is due to the fact that $K > 1$ below the axis of the sound channel where Thorp's measurements were made.

For the N Pacific case, the path integrated $K < 1$ and $\Delta \approx -4$ dB. However, the increase in K with depth below the thermocline causes losses to be greater than for the sound-channel mode. The axial value $K \approx 0.5$ would give $\Delta \approx -6$ dB for the same range. It should be pointed out that, in some areas where the K profiles do not fall off quite so rapidly with depth within the thermocline, $\Delta \rightarrow 0$ dB even when the minimum K value is the same. This indicates the very important effect of the K profile and the hazards of trying to use a regional average K for all ray paths.

For the Mediterranean case, $K > 1$ over the entire ray path and $\Delta \approx 12$ dB. The corresponding value for the Norwegian Sea, where K values are also fairly uniform but not as great, is $\Delta \approx 5$ dB. Note that CZ conditions are probable in both regions only during the summer months.

Bottom Bounce Mode

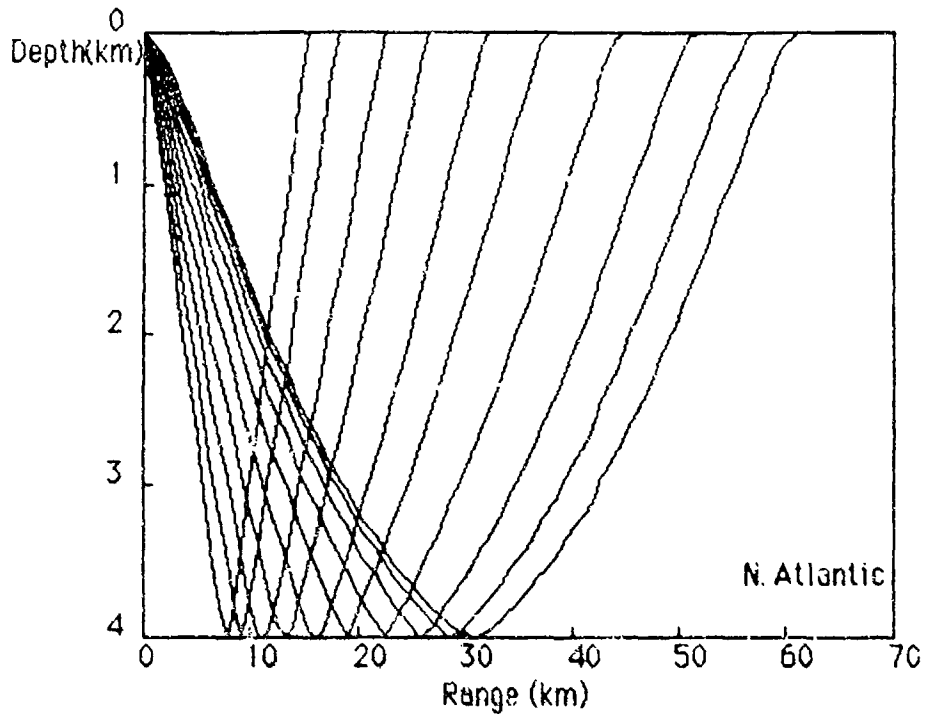


Figure 7: Bottom-bounce ray paths.

Bottom-bounce is important because it can be the only practical mode of operation at ranges between CZ zones when such conditions exist. Figure 7 shows some bottom-bounce ray paths for ranges out to the first CZ in the North Atlantic with water depth 4 km.

Tables 4-7 show calculations of the two-way path absorption for the four regions considered. Values for the K model, Thorp formula and the difference $\Delta = K_{\text{mod}} - \text{Thorp}$ are shown as a function of grazing angle and ray-range R (km). Note that K model values are approximately equal to the CZ values corrected in proportion to R . This is exactly true for the Thorp formula since the loss is independent of ray path.

Bottom grazing angles greater than about 5° are the main concern. For the N Atlantic, the 5° K model values are approximately 3.5 dB higher than Thorp. Corresponding Δ values are roughly -4.5 dB in the N Pacific, +9 dB in the E. Mediterranean and +7 dB in the Norwegian Sea. All values become small at high grazing angles because of the reduced ranges.

2Alpha(dB) BB N. Atl. 3.5kHz 4km depth				
Theta°	R(km)	Kmod	Thorp	Δ(dB)
5.3	62	32.1	28.7	3.4
7.2	58	30.0	26.7	3.3
10.0	53	27.1	24.1	3.0
14.0	46	23.5	20.9	2.7
18.8	39	19.9	17.6	2.3
24.0	33	16.9	15.0	1.9
30.0	27	14.0	12.4	1.6
36.0	23	11.7	10.4	1.3
42.1	19	9.5	8.5	1.1
47.5	16	8.1	7.2	0.9

Table 4. BB two-way path absorption/N. Atl.

2Alpha(dB) BB N. Pac. 3.5kHz 4km depth				
Theta°	R(km)	Kmod	Thorp	Δ(dB)
5.4	60	22.9	27.4	-4.5
9.2	53	20.2	24.1	-3.9
14.3	44	17.0	20.2	-3.2
19.5	37	14.2	16.9	-2.7
24.9	32	12.0	14.3	-2.3
30.8	26	9.9	11.7	-1.9
36.5	22	8.2	9.0	-1.6
41.9	19	7.1	8.5	-1.4
47.1	16	6.0	7.2	-1.1
51.7	15	5.5	6.5	-1.1

Table 5. BB two-way path absorption/N. Pac.

2Alpha(dB) BB E. Med. 3.5kHz 3km depth				
Theta°	R(km)	Kmod	Thorp	Δ(dB)
5.3	50	31.9	22.8	9.1
10.2	41	26.6	18.9	7.7
16.0	33	21.3	15.0	6.3
21.4	27	17.6	12.4	5.3
27.0	23	14.8	10.4	4.4
32.9	19	12.1	8.5	3.6
38.4	16	10.2	7.2	3.1
43.6	15	9.2	6.5	2.7
48.7	12	7.4	5.2	2.2
53.2	11	6.5	4.6	1.9

Table 6: BB two-way path absorption/E. Mediterranean

2Alpha(dB) BB 70N10E 3.5kHz 3km depth				
Theta°	R(km)	Kmod	Thorp	Δ(dB)
5.3	50	29.7	22.8	6.8
10.2	41	24.6	18.9	5.7
16.0	33	19.6	15.0	4.6
21.4	27	16.2	12.4	3.8
27.0	23	13.6	10.4	3.2
32.9	19	11.1	8.5	2.6
38.4	16	9.4	7.2	2.2
43.6	15	8.5	6.5	2.0
48.7	12	6.8	5.2	1.6
53.2	11	6.0	4.6	1.4

Table 7: BB two-way path absorption/Norwegian Sea

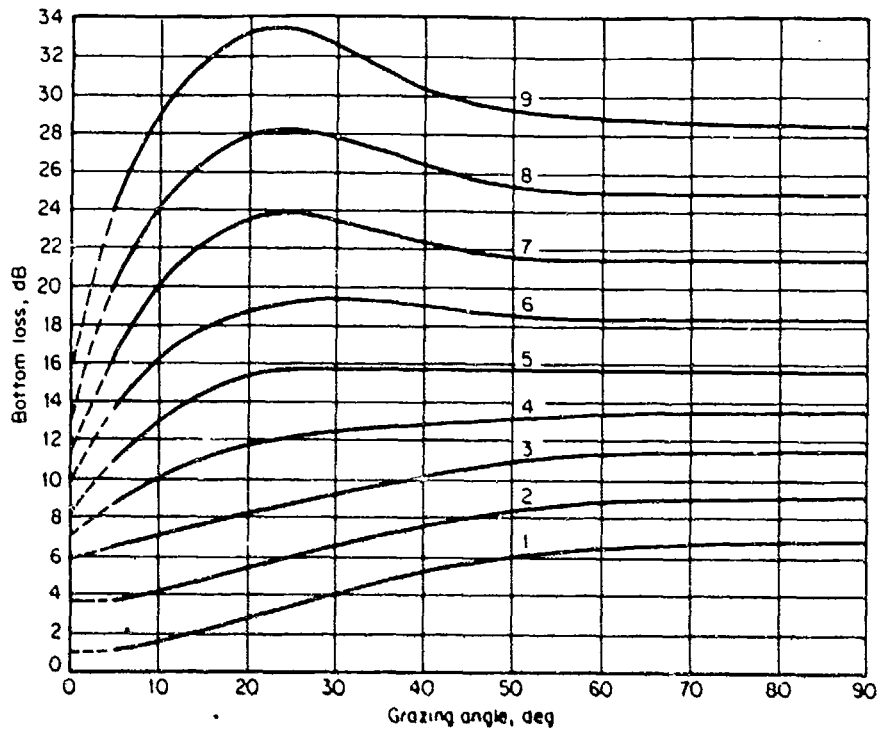


Figure 8: MGS Bottom loss model

Figure 8 shows the Marine Geophysical Survey bottom loss curves for the range 1-4 kHz [13]. Province numbers characteristic of the four regions are: N. Atlantic, #4; N. Pacific, #6, E. Mediterranean, #5, Norwegian Sea, #3.

The MGS data analysis was based on the Thorp formula and the question arises about the possible impact of the K model. A good indication of the approximate magnitudes can be seen from Δ values for the various regions. Since one-way paths were involved in the actual experiments, the Δ values in Tables 4-7 must be divided by two.

The results indicate that K model effects on MGS curves are significant at the lower grazing angles. In the Norwegian sea and E Mediterranean for example, bottom loss should be reduced by some 3-4 dB for 10°, which is roughly equivalent to one province number smaller. In the other regions, the corresponding values range within ± 2 dB. At the higher grazing angles, the shorter ranges tend to make the effects small in all cases.

Surface Duct Mode

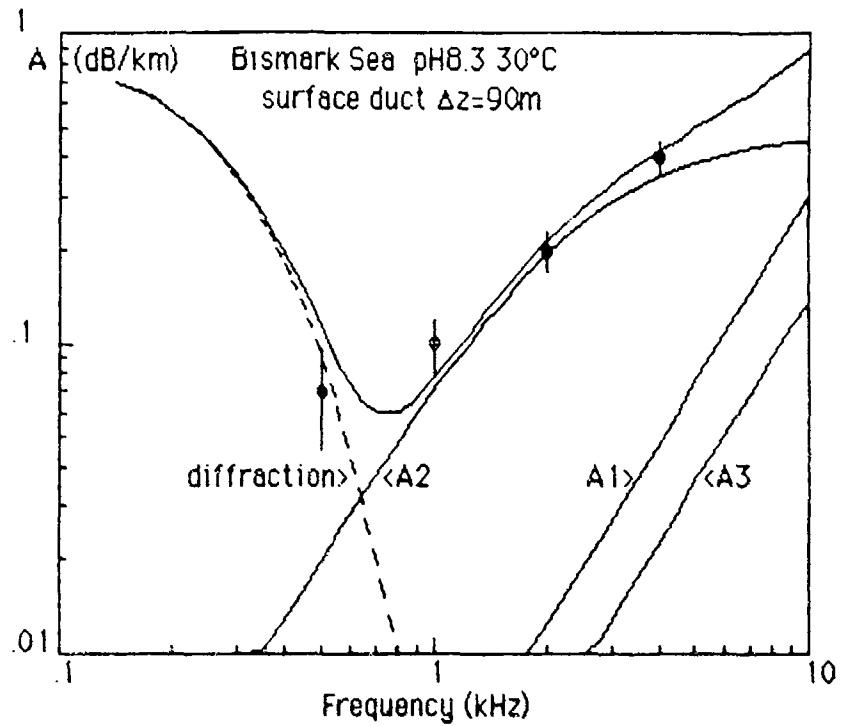


Figure 9: Bismark Sea surface-duct data and model.

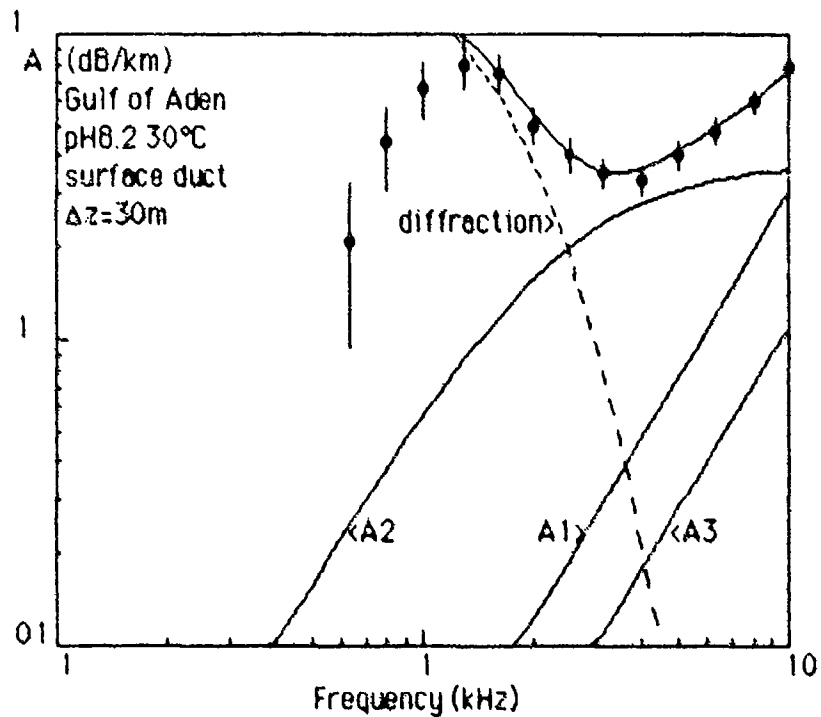


Figure 10 Gulf of Aden surface-duct data and model

Figures 9 and 10 show attenuation data from surface-duct experiments in the Bismark Sea and the Gulf of Aden [9] compared to the predictions of the K model. The diffraction loss for the lowest mode is calculated for a bilinear gradient with $g=0.18/s$ within the layer and a large negative gradient below. The three absorption components are identified and the top curve is the sum of the four components.

Since the model accounts for the experimental data above the diffraction cutoff in both cases, there are no extra loss that can be ascribed to surface reflection. This is not unexpected because the sea state was very low in both experiments.

2Alpha (dB) SD		Atl. 30°N	Pac. 45°N	E. Med.	70N10E
F (kHz)	R (km)	25	25	25	25
4.0	K mod.	20.1	19.7	21.9	17.6
	Thorp	13.8	13.8	13.8	13.8
	Δ	6.3 ± 0.9	5.8 ± 0.8	8.0 ± 0.9	3.7 ± 0.8
3.5	K mod.	18.1	17.3	19.6	15.1
	Thorp	11.7	11.7	11.7	11.7
	Δ	6.4 ± 0.8	5.6 ± 0.7	7.8 ± 0.8	3.4 ± 0.7
3.0	K mod.	16.0	15.1	17.3	12.9
	Thorp	9.8	9.8	9.8	9.8
	Δ	6.1 ± 0.7	5.2 ± 0.7	7.4 ± 0.8	3.0 ± 0.6
2.5	K mod.	13.5	12.9	14.8	10.7
	Thorp	8.2	8.2	8.2	8.2
	Δ	5.4 ± 0.6	4.7 ± 0.6	6.7 ± 0.7	2.6 ± 0.6
2.0	K mod.	10.7	10.6	12.1	8.7
	Thorp	6.6	6.6	6.6	6.6
	Δ	4.1 ± 0.5	4.0 ± 0.5	5.5 ± 0.6	2.1 ± 0.5

Table B: Two-way surface duct absorption.

Table B shows estimated two-way path absorption for 25 km target range. Note that the Δ values are all positive in this case because pH tends to be uniformly high near the surface.

Since surface loss must also be considered, the question then arises about the reliability of the prediction models.

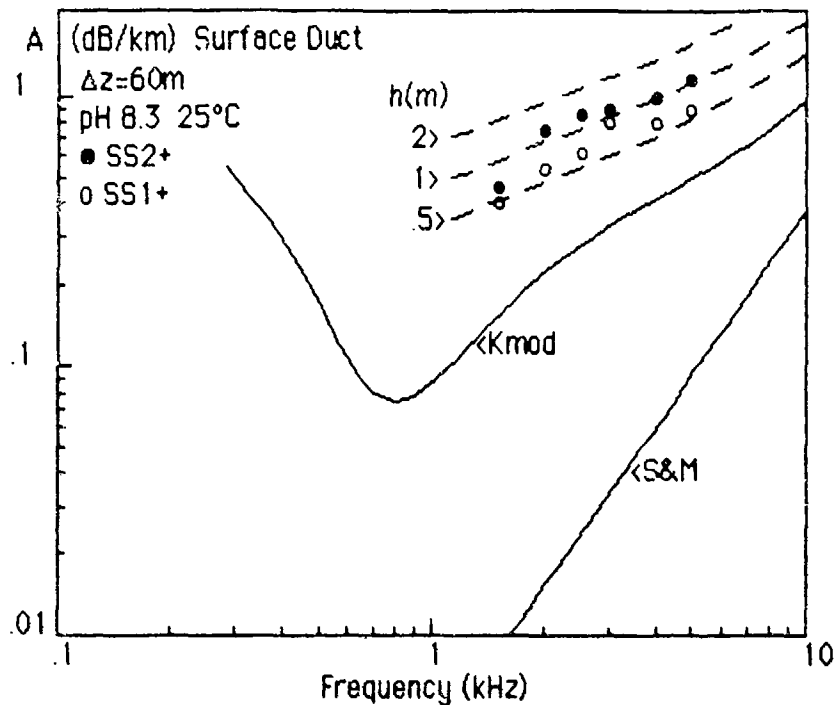


Figure 11: Comparison absorption and surface-loss formula.

The empirical surface-loss formula of Schulkin [14] is given by:

$$\alpha_s = 1.6(Fh)^{1/2} \text{ dB/limiting-ray cycle}$$

where F is in kHz and h is mean waveheight in ft. This formula was derived from analysis of AMOS [15] and other surface-duct experiments [16] by subtracting the S&M absorption formula [1] from the measured attenuation values, dividing the result by the skip distance of the limiting ray and curve-fitting the results.

Figure 11 compares the absorption predictions with attenuation estimates for a 60m surface duct. The data points are from ref. 16. To estimate the K model correction, the α_s and S&M formulae are added as shown by the dashed lines for wave heights $h=0.5, 1$ and 2 m. Subtracting the K model curve from these curves then gives corrected values of surface loss. Corrected values are therefore smaller by an amount equal to the difference between the two absorption formulae. In this example, the skip distance is roughly 6.3 km and the difference amounts to roughly 2 dB/bounce at 3.5 kHz. Since the K model and dashed curves are nearly parallel in this range, corrected values would become negative for $h < 0.15$ m, approximately.

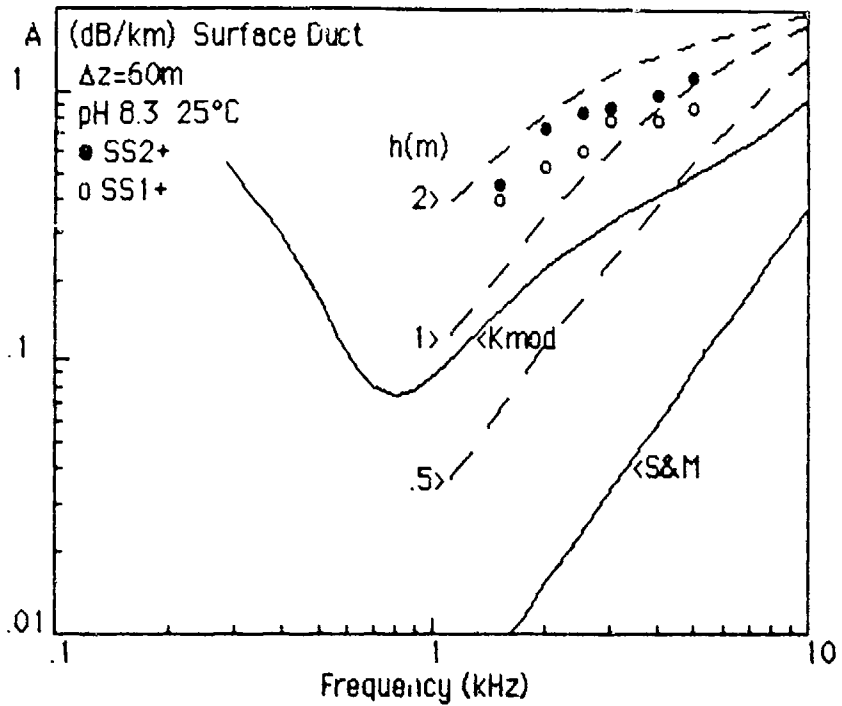


Figure 12: Comparison absorption and surface-loss formula.

Figure 12 compares the K-model predictions with estimates based on the empirical surface-loss formula currently used in the GENERIC Sonar Model:

$$\alpha_s = -20 \log_{10} (0.3 + 0.7 / [1 + (Fh/10)^2]) \text{ dB/limiting-ray cycle}$$

where F is in kHz and h is mean waveheight in ft. This formula is evidently a modified version of Beckmann-Spizzichino theory in which $\alpha_s \propto (Fh)^2$ for small parameter values. The modification causes asymptotic saturation at $\alpha_s \approx 10$ dB for high parameter values.

The dashed lines for wave heights h=0.5, 1 and 2m are again the sum of the S&M formula and α_s for the limiting ray in the 60m duct of Fig. 11. Where the values fall below the K model curve, correction would again yield negative values of surface loss.

It is clear that both surface-loss models tend to overestimate surface loss by a significant amount. However, it is difficult to see how the errors can be accurately assessed and corrected without going back to the original data (if still available!) and recalculating surface loss using the present absorption model.

Conclusion

This study has been limited mainly to the analysis of the potential impact of the K model on active sonar systems in the frequency range 3-4 kHz and on the surface and bottom-loss models used in performance prediction. The four regions examined are North Atlantic, North Pacific, Eastern Mediterranean and Norwegian Sea.

Comparison of K model predictions with those based on the Thorp formula indicates that two-way path loss in the CZ mode can vary from roughly 4 dB less in the N. Pacific to 12 dB more in the E. Mediterranean. Exact values can depend strongly on the K profile, particularly in the N. Pacific where the pH variations are greatest. The hazards of using regional average values of K for all ray paths have been pointed out.

In the bottom-bounce mode, the path loss is roughly equivalent to the CZ coefficient times operating range. Bottom reflection loss must, of course, be included. The MGS bottom-loss model examined here was based on analysis of one-way propagation experiments using the Thorp formula. In the Eastern Mediterranean, the corrected bottom loss for grazing angles near 10° is roughly equivalent to one province number less, the amount decreasing with increasing angle. In the other regions, the corresponding values are generally smaller.

The K model predictions for two-way path loss in the surface-duct mode at 3-4 kHz and 25 km vary from 3 to 8 dB greater than Thorp values because pH tends to be highest near the surface. The higher absorption clearly accounts for a large part of the observed excess attenuation that has previously been ascribed to surface loss. The surface-loss models are evidently all based on analyses of surface-duct experiments using pre-Thorp absorption models and predictions are both too high and not at all consistent. The difficulties in making appropriate corrections, particularly for other propagation modes, are obvious and a major reassessment of this problem is therefore indicated.

References

1. M. Schulkin and H. W. Marsh, "Sound absorption in sea water",
J. Acoust. Soc. Am. 34 864-865 (1962)
2. W. H. Thorp, "Deep ocean sound attenuation in the sub and low kilocycle-per-second region", J. Acoust. Soc. Am. 38, 648-654 (1965)
3. W. H. Thorp, "Analytic description of the low-frequency attenuation coefficient" J. Acoust. Soc. Am. 42 270-271 (1967)
4. C. C. Leroy, "Sound propagation in the Mediterranean Sea", in Underwater Acoustics, ed. V. M. Albers (Plenum, 1967)
5. E. Yeager, F. H. Fisher, J. Miceli and R. Bressel, "Origin of low-frequency sound absorption in sea water", J. Acoust. Soc. Am. 53, 1705-1707 (1973)
6. R. H. Mellen and D. G. Browning, "Variability of low-frequency sound absorption: pH dependence", J. Acoust. Soc. Am. 61, 704-706 (1977)
7. R. H. Mellen, D. G. Browning and V. P. Simmons, "Investigation of chemical sound absorption in sea water by the resonator method", J. Acoust. Soc. Am. 68, 248-257 (1980); 69, 1660-1662 (1981); 70, 143-148 (1981); 74, 987-993 (1983)
8. R. H. Mellen, V. P. Simmons and D. G. Browning, "Sound absorption in sea water: a third chemical relaxation", J. Acoust. Soc. Am. 65, 923-925 (1974)
9. R. H. Mellen, P. M. Scheifele and D. G. Browning, "Global model for sound absorption in sea water" NUSC Scientific and Engineering Studies, 1987.
10. F. H. Fisher and V. P. Simmons, "Sound absorption in sea water",
J. Acoust. Soc. Am. 62, 558-564 (1977)
11. World Ocean Atlas, edited by S. G. Gors'kov (Pergamon Press, New York)
Vol. 1, Pacific Ocean (1974); Vol. 2, Atlantic and Indian Oceans (1978);
Vol. 3, Arctic Ocean (1983)
12. GEOSECS Atlas, NSF (1981) Vol. 1, Atlantic Ocean; Vol. 3, Pacific Ocean;
Vol. 5, Indian Ocean
13. See R. J. Urick, Principles of Underwater Sound (McGraw-Hill, 1983)
14. M. Schulkin, "Surface-coupled losses in surface sound channels",
J. Acoust. Soc. Am. 44 1152-1154 (1968)
15. H. W. Marsh and M. Schulkin, "Report on the status of Project AMOS",
USL Rep. 155 A, 9 May 1967
16. H. R. Baker, A. G. Pieper and C. W. Searfoss, "Measurements of sound transmission loss at low frequencies 1.5-5 KC",
NRL Report 4225, Sept. 1953

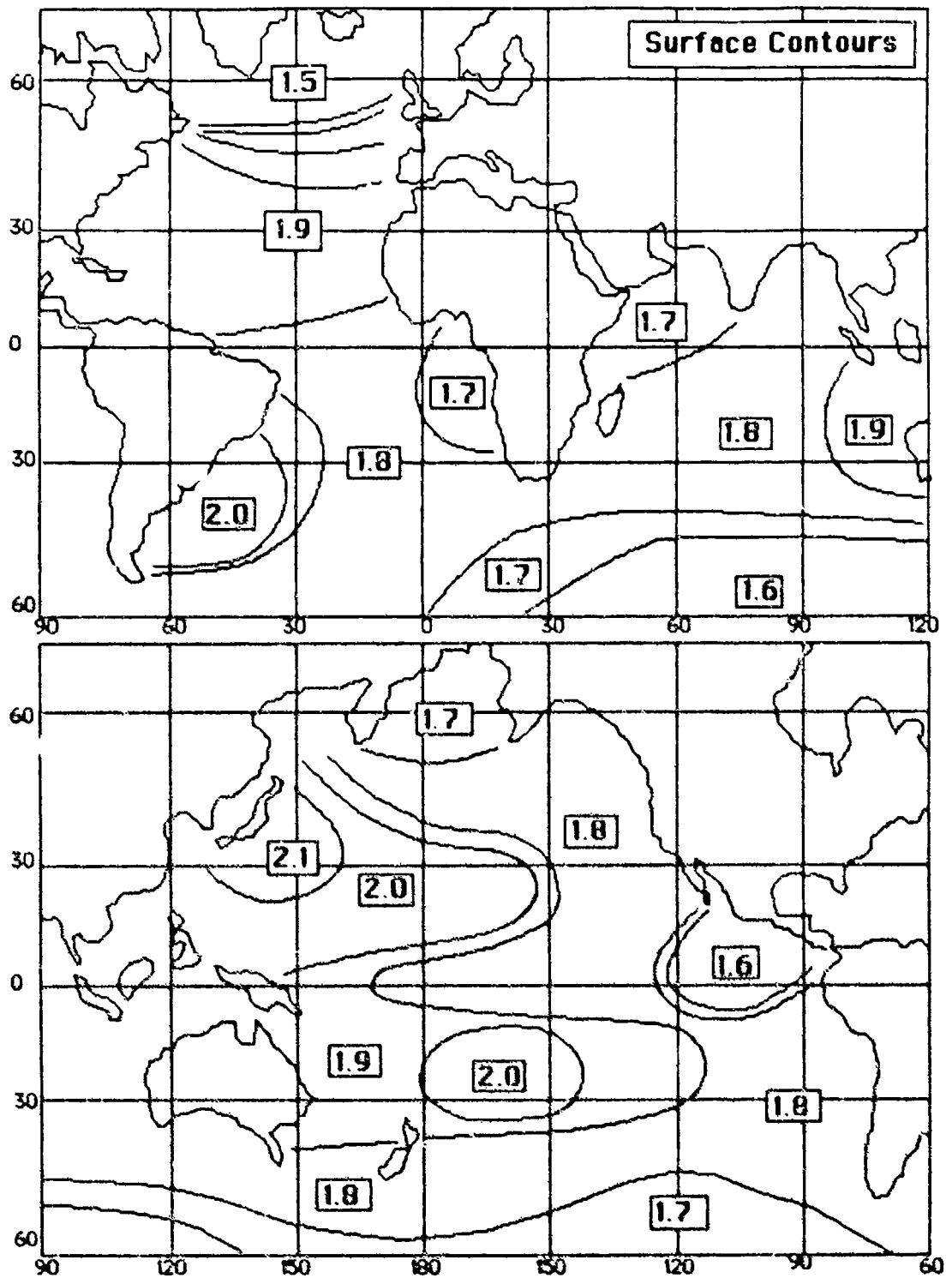


Figure 1A. Surface K Contours

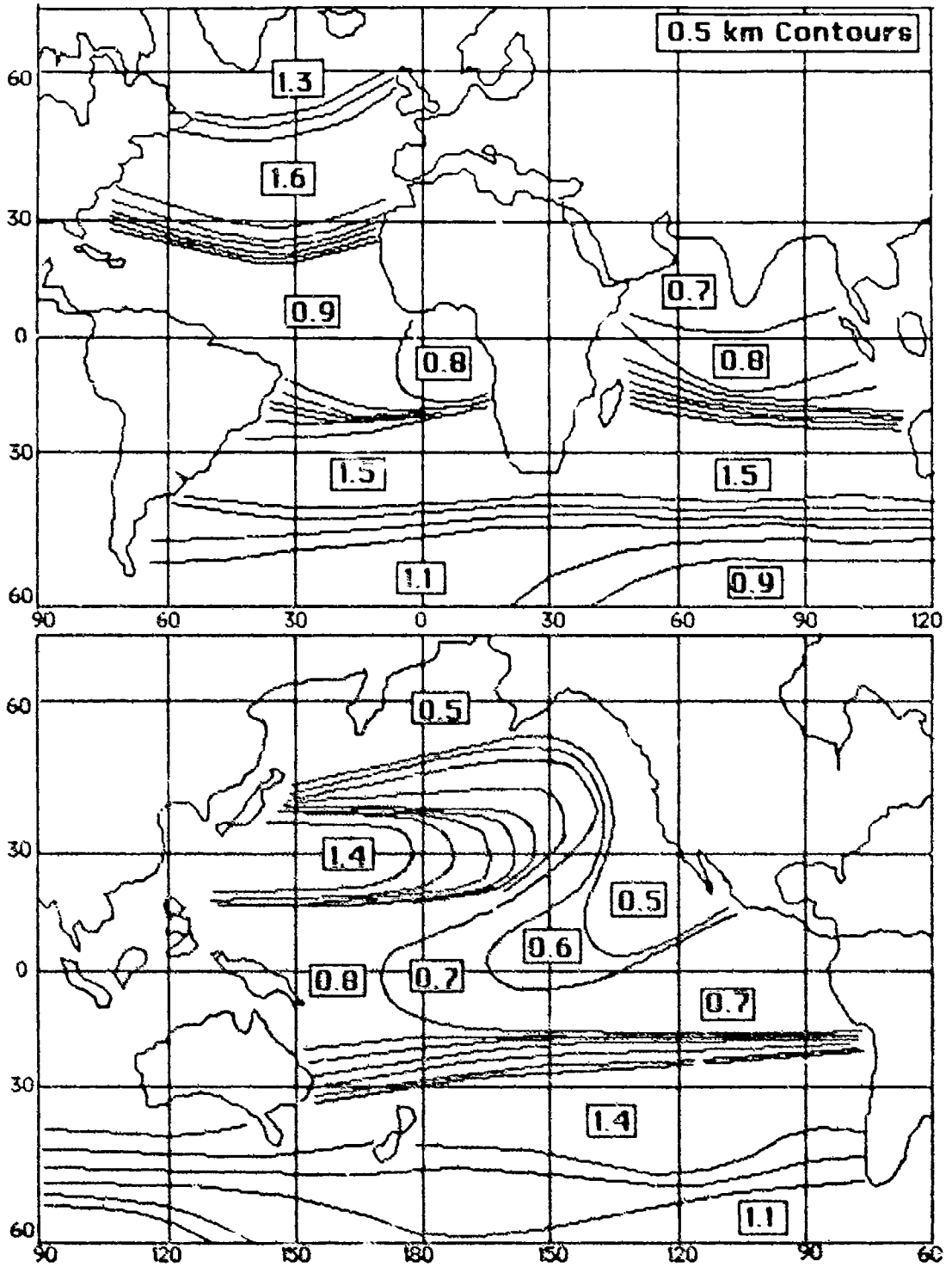


Figure 2A 0.5 km K Contours

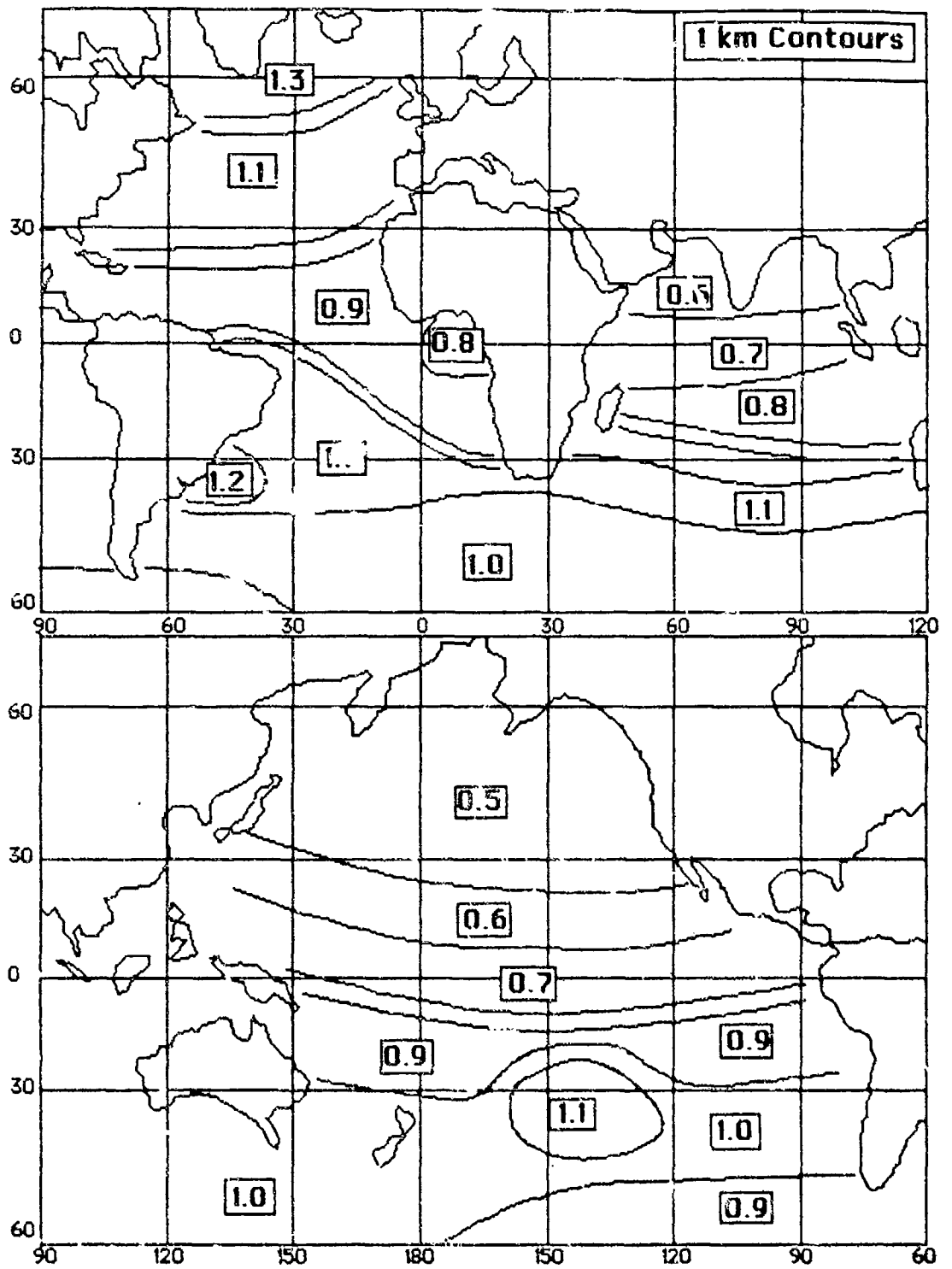


Figure 3A: 1 km K Contours

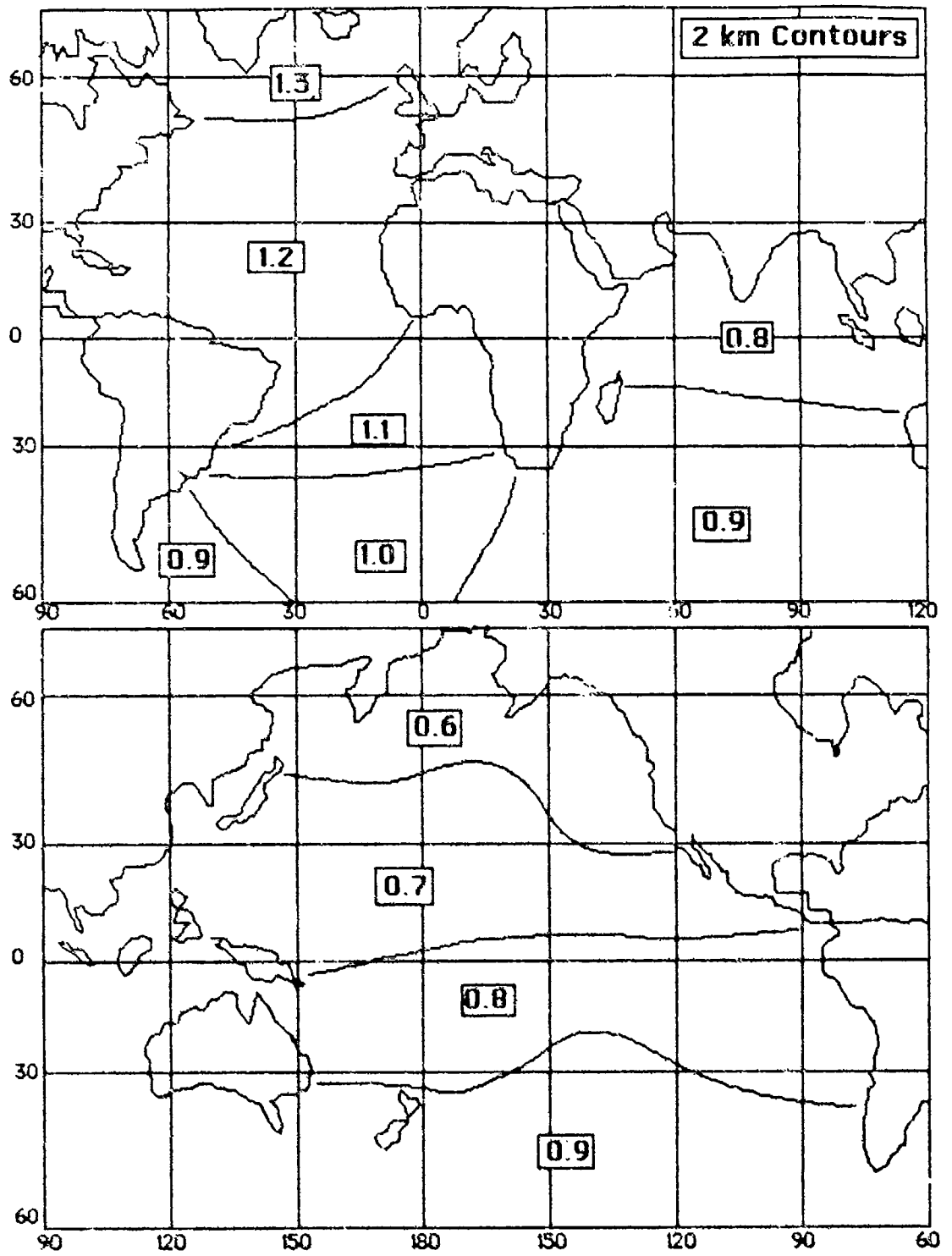


Figure 4A: 2 km K Contours

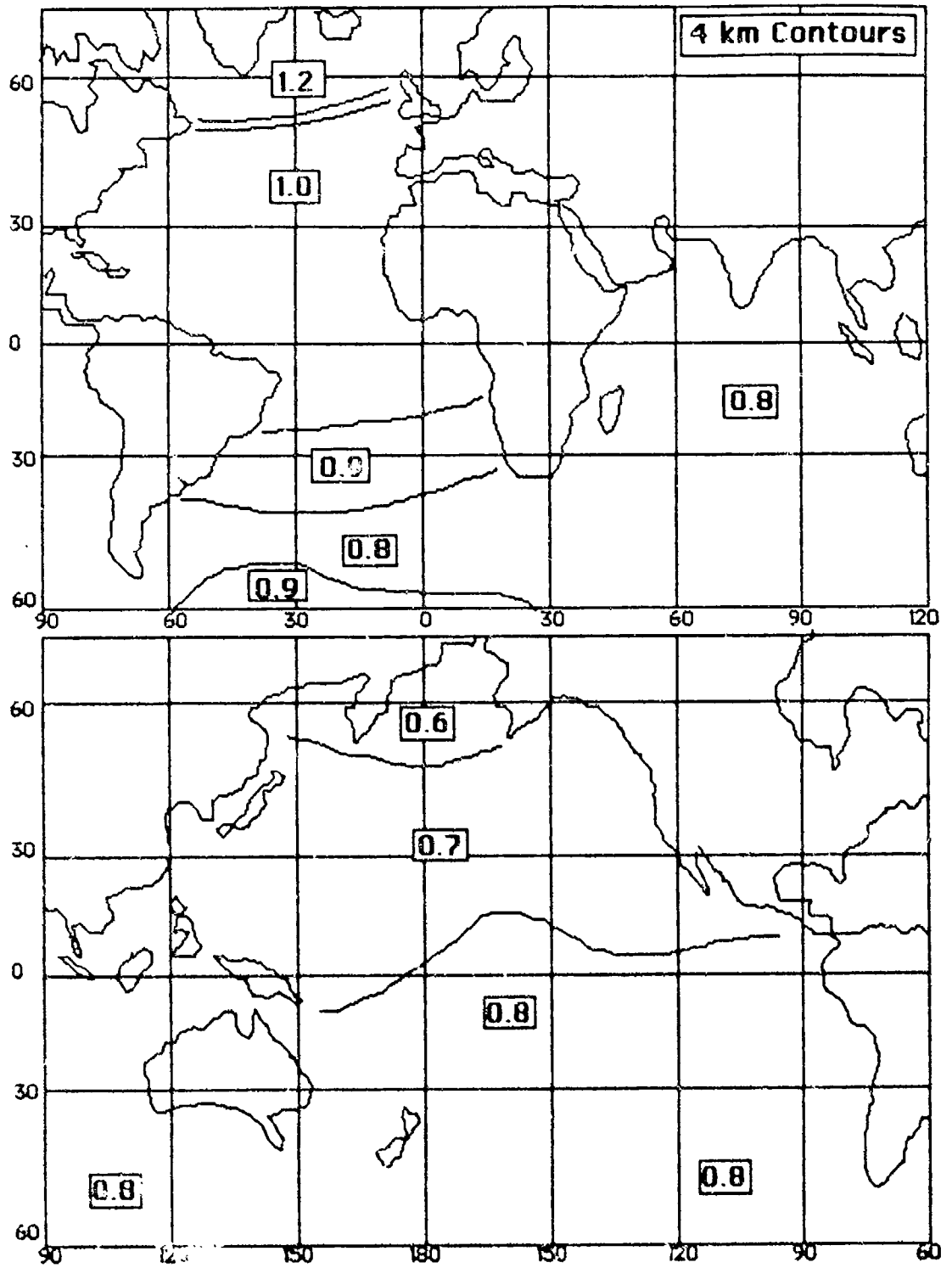


Figure 5A: 4 km K Contours

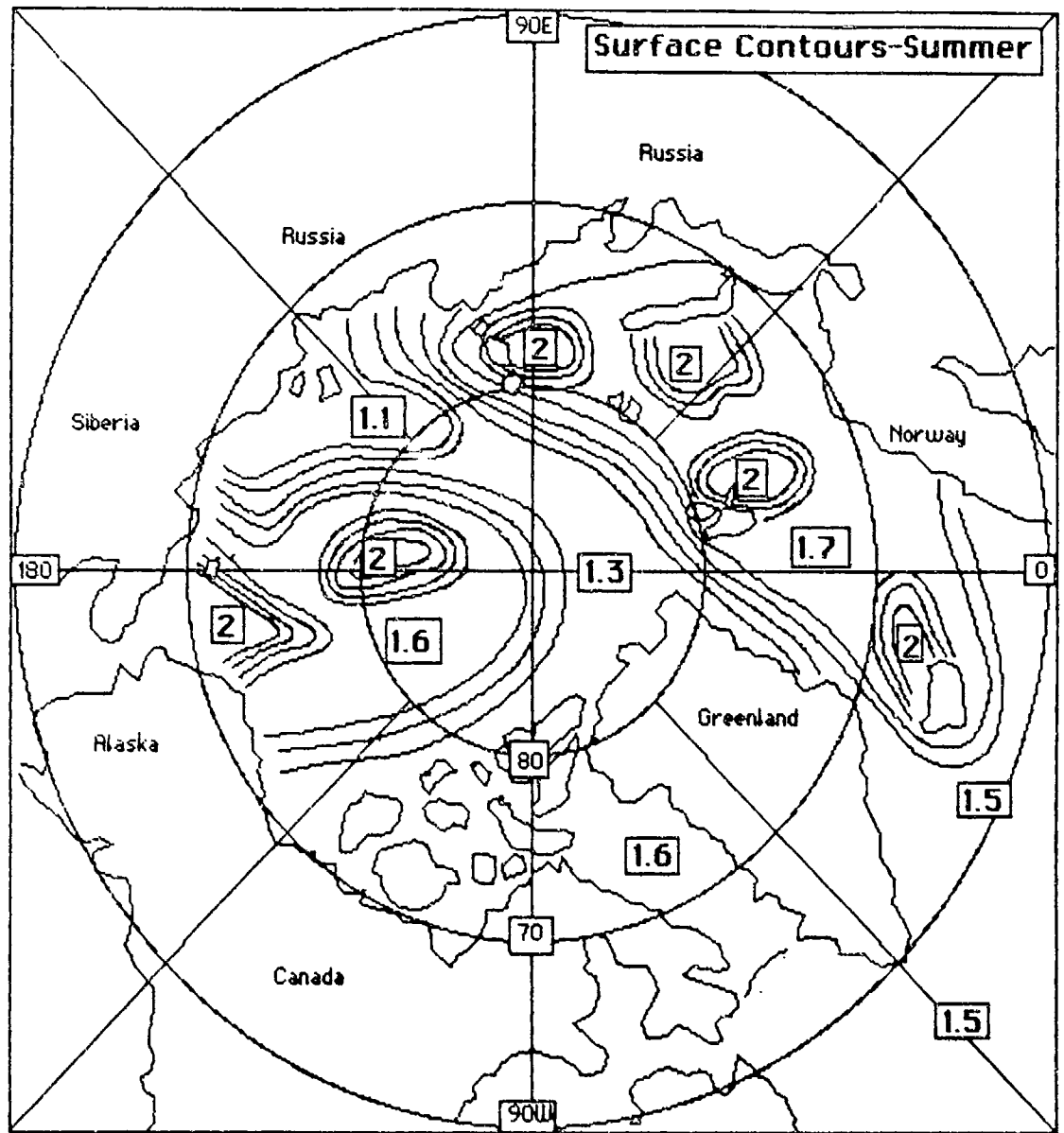


Figure 6A: Surface K contours-summer

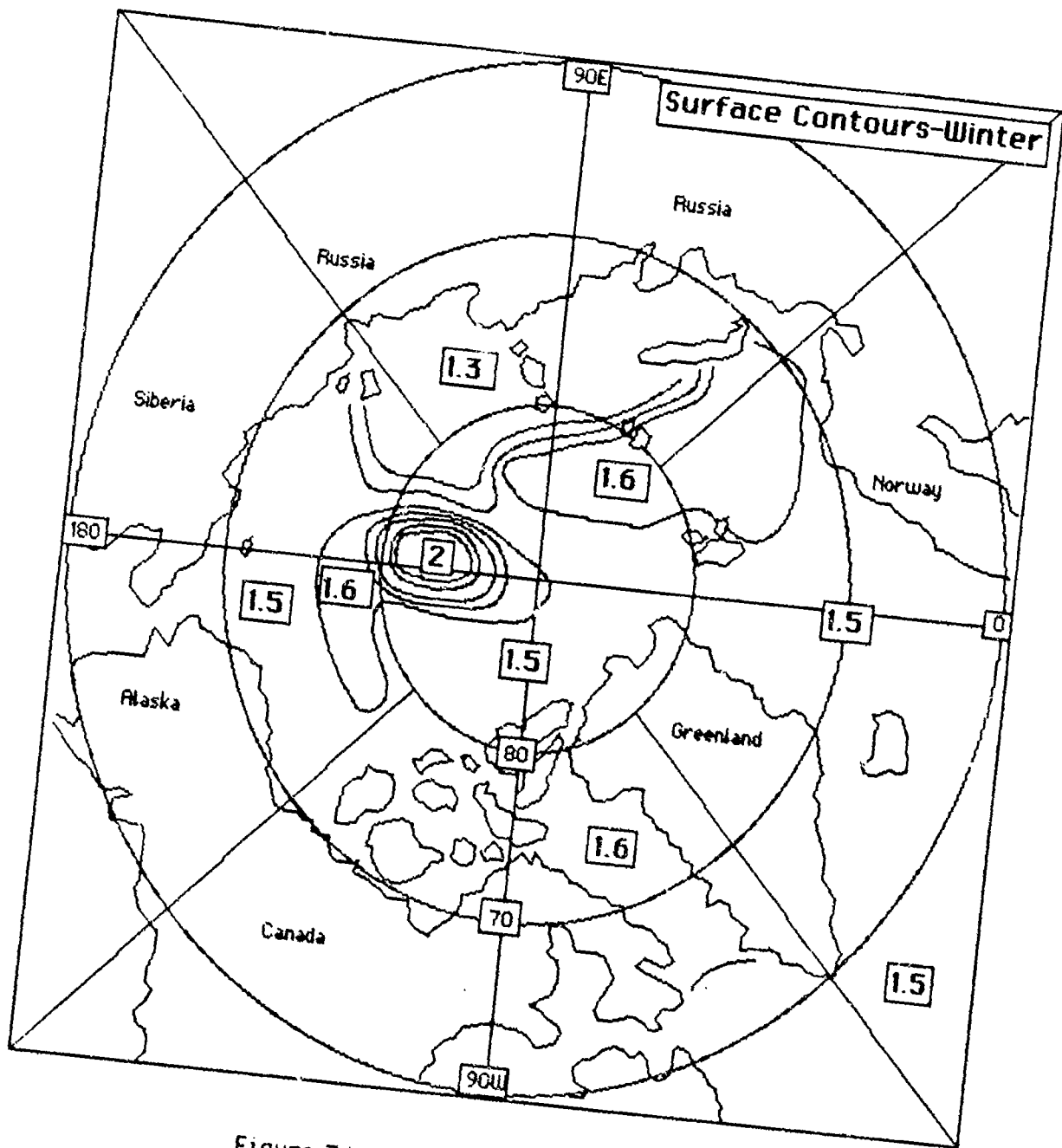


Figure 7A: Surface K contours-winter

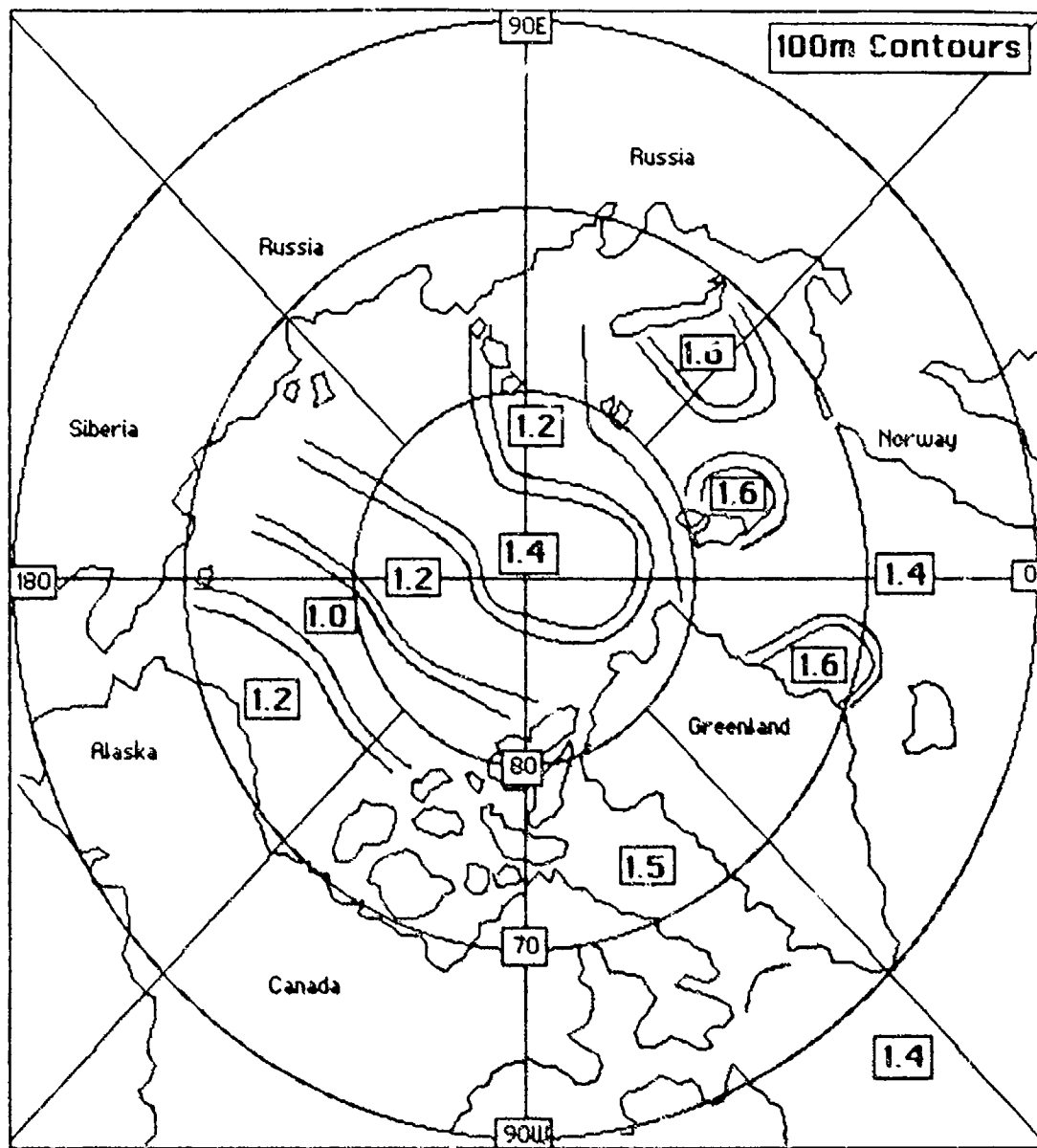


Figure 8A: 100m K contours

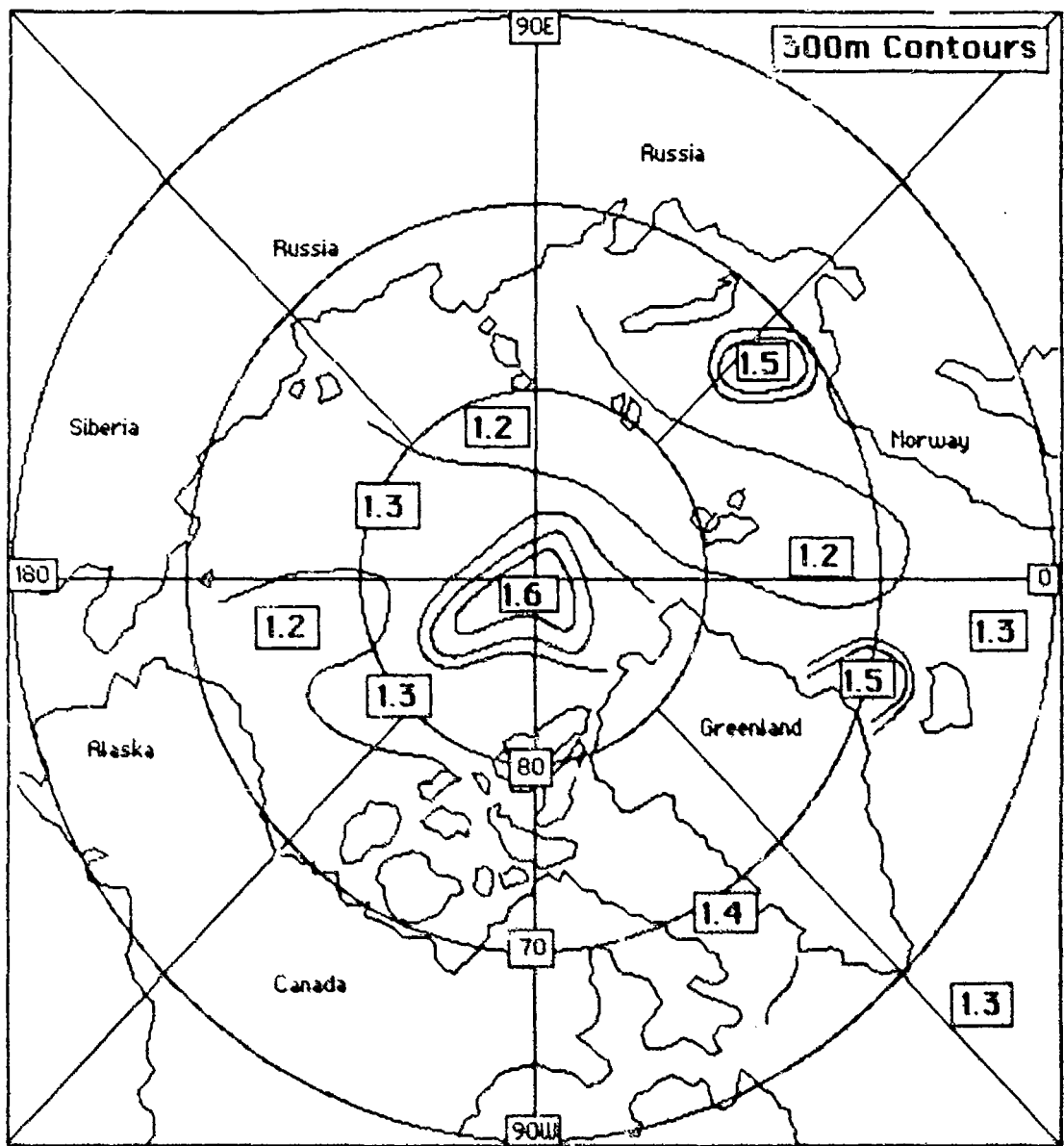


Figure 9A. 300m K contours

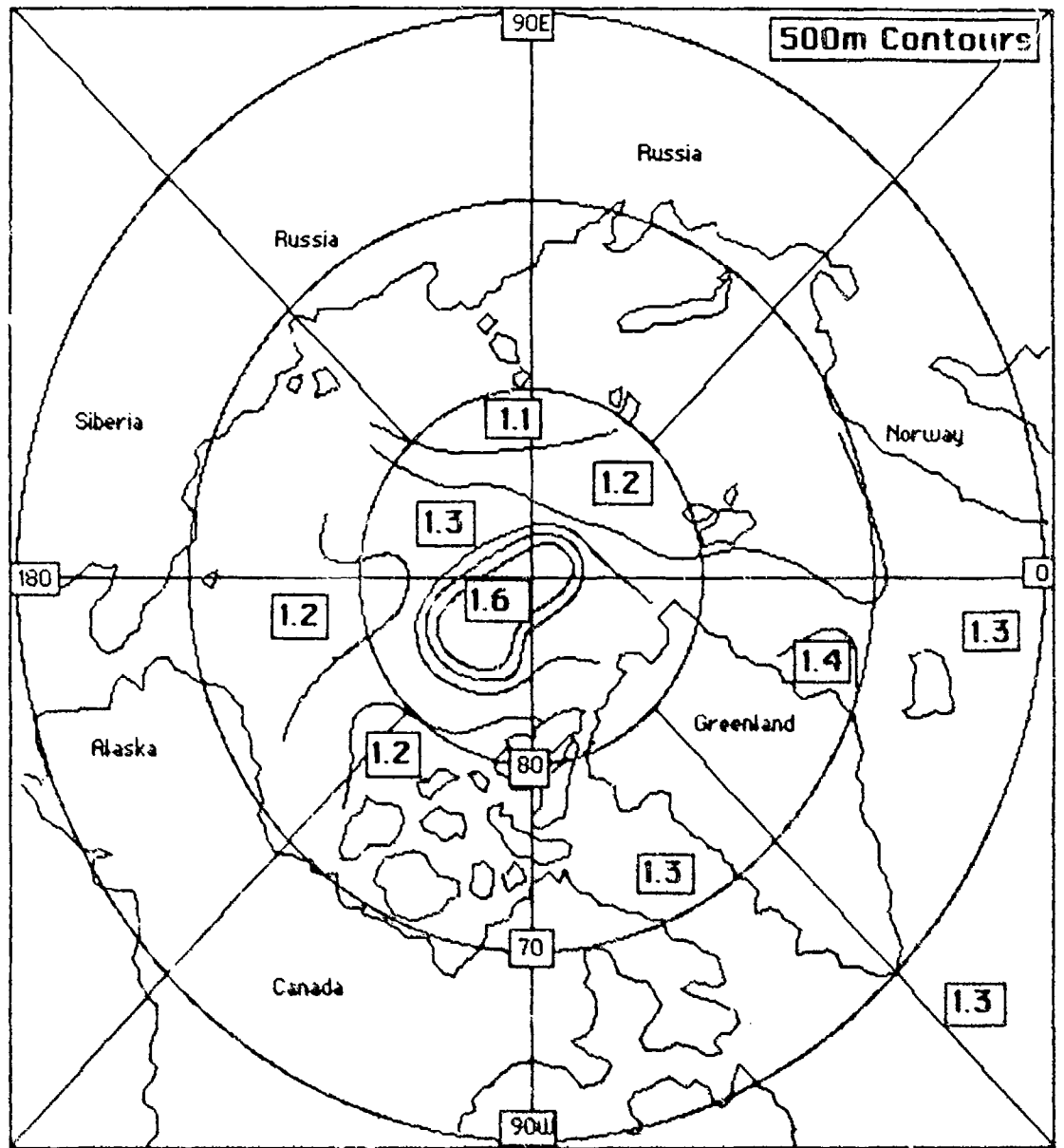


Figure 10A: 500m K contours

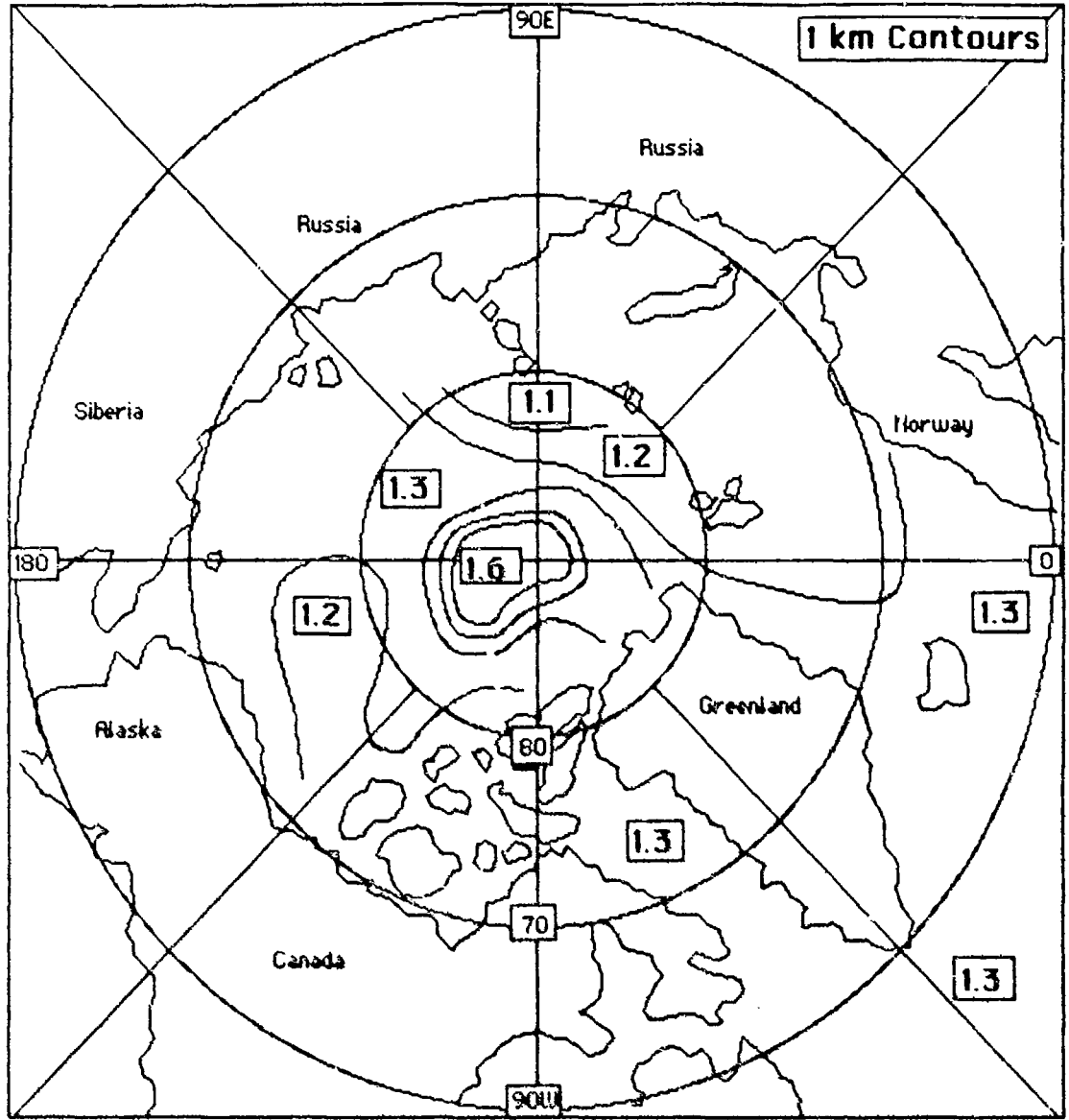


Figure 11A. 1 km K contours

INITIAL DISTRIBUTION LIST

Addressee	No. of Copies
CINCLANTFLT	1
CINPACFLT	1
COMMANDER SECOND FLT	1
COMMANDER THIRD FLT	1
COMMANDER SIXTH FLT	1
COMMANDER SEVENTH FLT	1
SURF FORCE LANT	1
SURF FORCE PAC	1
SUB FORCE LANT	1
SUB FORCE PAC	1
OPER T&E FORCE COMMANDER	1
SURF WARFARE DEV GROUP, NFOK	1
SUBMARINE DEV GROUP 1	1
SUBMARINE DEV SQUADRON 12	1
ASST SEC NAV (RES, ENG, & SYS)	1
DARPA	1
CNO (OP-71, -096, -098, -981, -02, -21, -22, -03, -35, -351)	10
CNR (OCNR-11, -12, -122, -13, -20)	5
ONR DET BAY ST. LOUIS	1
NAV AIR SYS COM (NAIR-03)	1
SPAWAR (PDW-80, -181, -183, -184)	4
NAVSEASYS COM (SEA-06, -62, -63, -63Y, PMS-396, -409, -411)	7
NRL	1
NORDA	1
NAV COASTAL SYS CTR	1
NO SC	1
NO SC DET HAWAII	1
DTNSROC	1
DTNSROC ACOS RES DET BAYVIEW	1
NSWC	1
NAVAL OCEANOGRAPHY COMMAND	1
NAVAL OCEANOGRAPHIC OFFICE	1
FLT NUMERICAL OCEANOGRAPHY CTR	1
NTSA	1
NPS	1
NWC	1
NTIC	1
CHA	1
DTIC	1